

## DETERMINATION OF THE TOTAL BREMSSTRAHLUNG PHOTON FLUX FROM ELECTRON ACCELERATORS BY SIMULTANEOUS ACTIVATION OF TWO MONITORS

*Tran Duc Thiep*<sup>a,1</sup>, *Truong Thi An*<sup>a</sup>, *Nguyen Tuan Khai*<sup>a</sup>,  
*Nguyen The Vinh*<sup>a</sup>, *Phan Viet Cuong*<sup>a</sup>,  
*Yu. P. Gangrski*<sup>b</sup>, *A. G. Belov*<sup>b</sup>, *O. D. Maslov*<sup>b</sup>

<sup>a</sup> Institute of Physics, VAST, Hanoi

<sup>b</sup> Joint Institute for Nuclear Research, Dubna

We have determined the total bremsstrahlung photon fluxes with end-point energies in the giant dipole resonance (GDR) region produced by the electron accelerator Microtron MT-25 (Flerov Laboratory of Nuclear Reactions, Joint Institute for Nuclear Research, Dubna) and that of 65 MeV bremsstrahlung produced by the linear electron accelerator (Pohang Neutron Facility, Pohang, South Korea). The method we used was the photon activation technique. To ensure the accuracy of the results, we carried out simultaneous photon activation of two monitors made of Cu and Au foils in the same irradiation conditions. The results are discussed in the paper.

Определяются полные потоки тормозных фотонов с целевыми энергиями в области гигантского дипольного резонанса (ГДР), возникающие на электронном ускорителе микротрон МТ-25 (Лаборатория ядерных реакций им. Г. Н. Флерова, Объединенный институт ядерных исследований, Дубна), а также потоки в тормозном излучении при 65 МэВ, образующиеся на линейном электронном ускорителе (пхоханский нейтронный ускоритель, Пхохан, Южная Корея). Использовался метод фотонной активации. Для обеспечения точности результатов была проведена одновременная фотонная активация двух мониторов, сделанных из медной и золотой фольги в одинаковых радиационных условиях. Представлено также обсуждение полученных результатов.

PACS: 10.25.20.-x

### INTRODUCTION

Recently, electron accelerators have been widely used in different fields of fundamental research and practical applications [1–5]. Although electron accelerators are equipment which accelerates electrons, in fact they are intense sources of bremsstrahlung photon and photon-neutron beams. The principle of converting the electrons into bremsstrahlung can be found in [6]. The bremsstrahlungs have become a powerful tool for studying different kinds of photonuclear reactions and nuclear mechanism including nuclear resonance fluorescence [1], photofission [2] and excitation of nuclear states [3]. Medical and industrial applications of

---

<sup>1</sup>Tel.: +84.983201915; e-mail: tdthiep@iop.vast.ac.vn

bremsstrahlung can be found in [4,5]. For an electron accelerator, the determination of bremsstrahlung photon flux is of important significance. The bremsstrahlung photon flux allows us (a) to determine the characteristics of photonuclear reaction as the cross section and yield [7–9], (b) to estimate the possibility of producing the neutron-rich radioactive nuclei beam [10, 11] and photoneutron beam [12, 13] for fundamental research, and (c) to determine the sensitivity of photon activation method [14, 15] and the possibilities for radiation protection and shielding [16]. For radiation protection, the usually used unit for bremsstrahlung photon flux measurement is  $10^{-2} \text{ Gy} \cdot \text{m}^{-2} \cdot \text{min}^{-1}$  or  $\text{rad} \cdot \text{m}^{-2} \cdot \text{min}^{-1}$  [16]. However, in photonuclear reaction investigation and photon activation method, it is more proper to use unit photon,  $\text{cm}^{-2} \cdot \text{s}^{-1} \cdot \mu\text{A}^{-1}$ , i.e., the number of photons passing  $1 \text{ cm}^2$  in 1 s for an electron beam of  $1 \mu\text{A}$ .

In this paper, we present the results of determination of total photon fluxes of the bremsstrahlungs with end-point energies of 15, 18, 22 and 24 MeV produced by the Microtron MT-25 and that of 65 MeV bremsstrahlung of Pohang electron accelerator.

## 1. METHOD TO DETERMINE THE TOTAL BREMSSTRAHLUNG PHOTON FLUX

In order to determine the total bremsstrahlung photon flux, we applied the photon activation method in our experiments.

**1.1. The Basis of the Activation Method.** During the activation process, the number of radioactive nucleus  $N(t)$  formed at moment  $t$  can be described as follows:

$$\frac{dN(t)}{dt} = N_0 \sigma(E) \phi(E) - \lambda N(t). \quad (1)$$

By resolving Eq. (1) for the case of activation with bremsstrahlung photon flux, we obtained the following expression for the number of gamma rays of interest irradiated from the radioactive nucleus:

$$\begin{aligned} S &= \frac{m\theta N_A \varepsilon I}{M\lambda} (1 - e^{-\lambda t_i}) e^{-\lambda t_d} (1 - e^{-\lambda t_m}) \int_{E_{\text{th}}}^{E_m} \sigma(E) \phi(E, E_m) dE = \\ &= \frac{m\theta N_A \varepsilon I (1 - e^{-\lambda t_i}) e^{-\lambda t_d} (1 - e^{-\lambda t_m}) \sigma_{\text{int}} \phi_{\text{th}}}{M\lambda(E_m - E_{\text{th}})}, \quad (2) \end{aligned}$$

where  $E_m$  is the bremsstrahlung end-point energy;  $\phi(E, E_m)$  is the bremsstrahlung photon flux at energy  $E$ ;  $\sigma(E)$  is the cross section for the radioactive nucleus, i.e., the giant resonance curve;  $\phi_{\text{th}} = \int_{E_{\text{th}}}^{E_m} \phi(E, E_m) dE$  is the bremsstrahlung photon flux for the region from reaction

threshold  $E_{\text{th}}$  to end-point energy  $E_m$ ;  $\sigma_{\text{int}} = \int_{E_{\text{th}}}^{E_m} \sigma(E) dE$  is the integrated cross section for the same region;  $S$  is the area under the photopeak of interest characterizing the radioactive nucleus, i.e., the number of gamma rays;  $t_m$  is the measurement time;  $t_i$  is the irradiation

time;  $t_d$  is the decay time;  $m$  is the elemental mass;  $\theta$  is the isotope abundance;  $N_A$  is Avogadro number;  $M$  is atomic mass;  $I$  is the gamma ray intensity, and  $\varepsilon$  is the detector efficiency.

The value of  $\phi_{\text{th}}$  can be determined from expression (2) as follows:

$$\phi_{\text{th}} = \frac{SM\lambda(E_m - E_{\text{th}})}{(1 - e^{-\lambda t_i}) e^{-\lambda t_d} (1 - e^{-\lambda t_m}) \sigma_{\text{int}} m\theta N_A \varepsilon I}. \quad (3)$$

In expression (3) all parameters are well known from the literature [17, 19, 20] and experiment, except the integrated cross section  $\sigma_{\text{int}}$ . Therefore, it is necessary to calculate  $\sigma_{\text{int}}$  in order to determine  $\phi_{\text{th}}$ . Besides, as mentioned above,  $\phi_{\text{th}}$  is the bremsstrahlung photon flux for the region from  $E_{\text{th}}$  to  $E_m$ . However, our purpose was to determine the total bremsstrahlung photon flux  $\phi = \int_0^{E_m} \phi(E, E_m) dE$ , i.e., for the energy region from 0 to  $E_m$ . In order to do this, it was necessary to know the energy distribution of bremsstrahlung.

**1.2. Calculation of the Integrated Cross Section.** In photonuclear reactions the giant resonance curves  $\sigma(E)$  have Lorentz form. In order to calculate the integrated cross section, we transformed the integral into a sum in which the energy interval  $(E_m - E_{\text{th}})$  was divided into 1000 subintervals as follows:

$$\sigma_{\text{int}} = \int_{E_{\text{th}}}^{E_m} \sigma(E) dE = \int_{E_{\text{th}}}^{E_m} \frac{\sigma_0 \Gamma^2 E^2}{(E_0^2 - E^2)^2 + \Gamma^2 E^2} dE = \sum_{i=1}^{1000} \frac{\sigma_0 \Gamma^2 E_i^2}{(E_0^2 - E_i^2)^2 + \Gamma^2 E_i^2} \Delta E_i, \quad (4)$$

where  $\sigma_0$  is the maximum cross section at energy  $E_0$  and  $\Gamma$  is the width of the giant resonance curve;  $E_{\text{th}}$  is the reaction threshold and  $\Delta E_i = (E_m - E_{\text{th}})/1000$ .

The integrated cross section was calculated by using computational program Mathematica presented in [18]. The calculations show that the energy interval  $(E_m - E_{\text{th}})$  was unnecessary to be divided into more than 1000 subintervals.

**1.3. Calculation of the Energy Distribution of Bremsstrahlung.** The energy distribution of bremsstrahlung photon flux can be estimated by the Schiff approximation [23] or simulation method. In our work we used the simulation method presented in [24–26].

## 2. EXPERIMENTAL

In our experiment to determine the bremsstrahlung photon fluxes with end-point energy in the GDR region, monitors made of Au and Cu foils were simultaneously irradiated under the same irradiation conditions. Figure 3 shows the experimental arrangement at the Microtron MT-25. In the case of 65 MeV bremsstrahlung of the Pohang electron linear accelerator, the experimental arrangement was similar, but only Cu monitor was used. The photonuclear reactions  $^{197}\text{Au}(\gamma, n)^{196m,g}\text{Au}$  and  $^{65}\text{Cu}(\gamma, n)^{64}\text{Cu}$  were used for the calculations. The parameters of the giant resonance curves for these reactions which were taken from [17] are shown in Table 1 and Figs. 1, 2. Table 2 shows the decay characteristics of the nuclei of interest [19, 20].

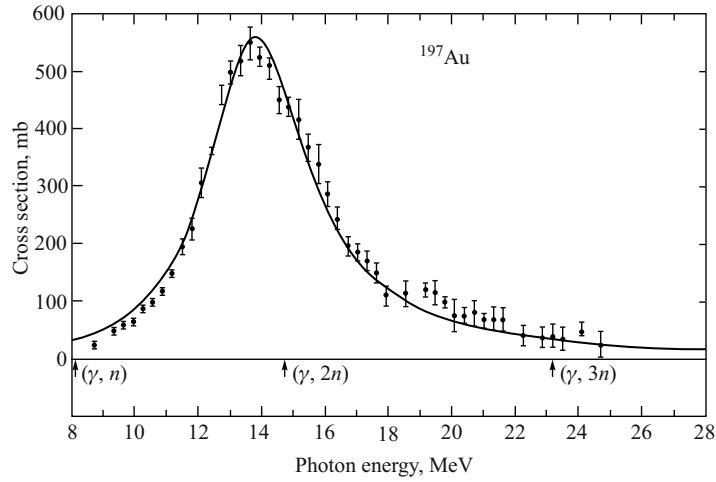
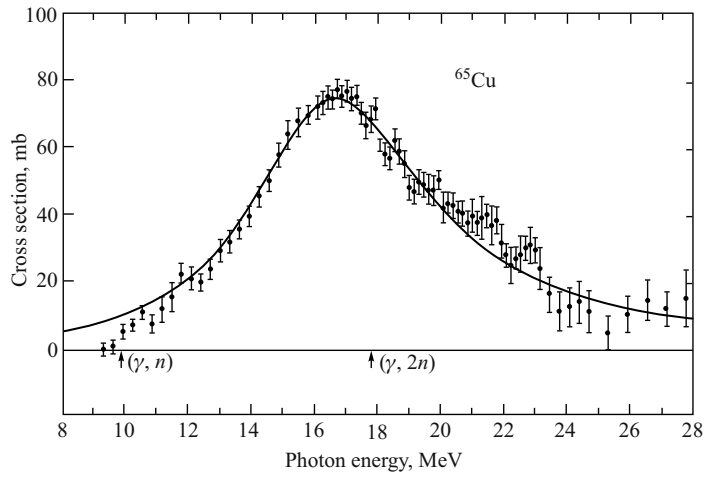

 Fig. 1. The giant resonance curve of  $^{197}\text{Au}$ 

 Fig. 2. The giant resonance curve of  $^{65}\text{Cu}$ 

Table 1. Characteristics of some nuclei which can be used for the experiment

Quantity	Nucleus						
	$^{65}\text{Cu}$	$^{90}\text{Zr}$	$^{124}\text{Sn}$	$^{135}\text{Ba}$	$^{143}\text{Nd}$	$^{197}\text{Au}$	$^{208}\text{Pb}$
$E_0$ , MeV	16.70	16.5	15.19	15.26	15.01	13.82	13.46
$\sigma_0$ , mb	75.20	185.00	283.00	327.00	349.00	560.00	491.00
$\Gamma$ , MeV	6.89	4.02	4.81	4.61	4.75	3.84	3.90
$E_{\text{th}}$ , MeV	9.90	12.00	8.50	8.60	6.10	8.10	7.40

*Note:*  $\sigma_0$  is the maximum cross section at energy  $E_0$  and  $\Gamma$  is the width of the giant resonance curve;  $E_{\text{th}}$  is the reaction threshold.

Table 2. The decay characteristics and gamma rays of the nuclei of interest

Nuclear reactions	Reaction product	Abundance, %	Half-life	Reaction threshold, MeV	Mass, g. mol	Gamma energy, keV and intensity, %
$^{197}\text{Au}(\gamma, n)^{196m,g}\text{Au}$	$^{196g}\text{Au}$	100	6.183 d	8.10	196.967	333.00(24.40) 355.73(93.60)
$^{65}\text{Cu}(\gamma, n)^{64}\text{Cu}$	$^{64}\text{Cu}$	30.90	12.7 h	9.90	63.54	511.00(37.00) 1345.76(0.48)

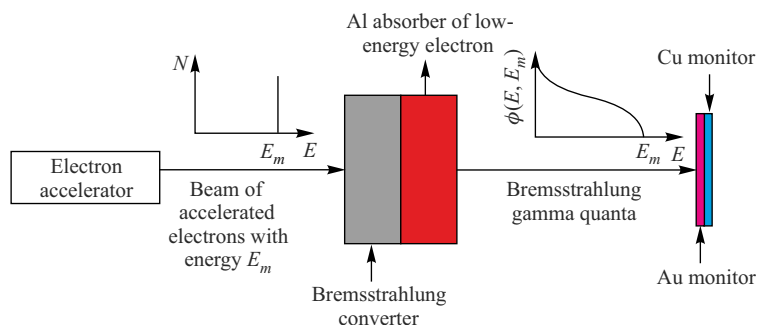


Fig. 3. Experimental arrangement at Microtron MT-25

**2.1. Monitor Preparation and Irradiation.** We used monitors made of natural gold (Au) and copper (Cu) foils in circle form of 1 cm diameter. The parameters of monitors and the irradiation procedure are shown in Table 3. The description of the Microtron MT-25 and its characteristics are presented in [21]. The essential advantage of this Microtron is the small energy spread of the accelerated electrons (30–40 keV) at high beam intensity (up to an average power of 600 W). This allows the measurement of the total bremsstrahlung photon flux at strictly definite end-point energy. The electron–photon converter was W disk 4 mm thick, cooled by water. To absorb low-energy electrons passing the converter in the monitors, an aluminum screen 20 mm thick was placed behind the converter. The bremsstrahlung end-point energy of this accelerator may vary stepwise from 10 to 25 MeV, i.e., over the GDR

Table 3. The parameters of monitors and the irradiation procedure

Bremsstrahlung end-point energy, MeV	Monitor type	Purity, %	Monitor mass, g	Electron beam, $\mu\text{A}$	Irradiation time, min
15	Au	99.99	0.1954	12	40
	Cu	99.99	0.1495	12	40
18	Au	99.99	0.2190	10	30
	Cu	99.99	0.1303	10	30
22	Au	99.99	0.2977	15	10
	Cu	99.99	0.1411	15	10
24	Au	99.99	0.2157	15	20
	Cu	99.99	0.1545	15	20
65	Au	99.99	0.0361	0.6	120
	Cu	99.99	0.0369	0.6	120

region. The Au and Cu monitors were placed closely to each other at a distance of 1 cm from the Al absorber. In the case of 65 MeV bremsstrahlung of the linear electron accelerator, the irradiation time and the average electron beam were 240 min and 0.6  $\mu\text{A}$ , respectively. This accelerator operated with a repetition rate of 10 Hz, a pulse width of 1.2  $\mu\text{s}$  and a pulse electron beam of 50 mA. Its description can be found in [22]. The Cu monitor was placed at a distance of 2.5 cm from the Al absorber.

**2.2. Gamma Spectra Measurement.** The gamma spectra of the monitors irradiated in both institutes were measured with spectroscopic systems consisting of an 8192 channel analyzer and a high-energy resolution (180 keV at gamma ray 1332 keV of  $^{60}\text{Co}$ ) HP(Ge) semiconductor detector Canberra. The GENIE2000 (Canberra) computer program was used for data processing. The efficiencies of the detectors were determined with a set of standard single gamma ray sources calibrated to 1–2 %.

### 3. RESULTS AND DISCUSSION

**3.1. The Integrated Cross Sections.** The integrated cross sections of  $^{197}\text{Au}(\gamma, n)^{196m,g}\text{Au}$  and  $^{65}\text{Cu}(\gamma, n)^{64}\text{Cu}$  reactions from the threshold energy to the bremsstrahlung end-point energies are presented in Table 4.

Table 4. The integrated cross sections (in mb · MeV) from the threshold energy to bremsstrahlung end-point energies

Nuclei	Bremsstrahlung energy, MeV									
	15	17	18	19	20	21	22	23	24	65
$^{65}\text{Cu}$	142.3	282.9	354.1	414.3	462.3	500.0	529.8	553.8	573.3	734.7
$^{197}\text{Au}$	1819.3	2368.0	2511.2	2613.0	2689.2	2748.4	2796.0	2835.2	2868.2	—

**3.2. The Energy Distribution of Bremsstrahlungs.** Table 5 shows the results calculated in % for 15, 18, 22 and 24 MeV end-point energies. For 65 MeV bremsstrahlung, the contribution of photon flux from 0 to  $E_{\text{th}} = 9.90$  MeV of  $^{65}\text{Cu}$  was 76.83 % and from 9.90 to 65 MeV was 23.17 %.

Table 5. Energy distributions of bremsstrahlung with different end-point energies

Energy region, MeV	15 MeV, %	18 MeV, %	22 MeV, %	24 MeV, %
0–2	64.99	61.85	56.24	55.57
2–4	16.98	16.20	16.35	16.28
4–6	8.04	8.20	8.47	8.50
6–8	4.83	5.10	5.36	5.40
8–10	2.91	3.15	3.63	3.61
10–12	1.64	2.12	2.85	2.89
12–15	0.63	2.54	2.96	3.15
15–18		0.84	1.94	2.30
18–20			1.05	1.14
20–22			0.43	0.62
22–24				0.27

**3.3. The Total Bremsstrahlung Photon Fluxes.** Figures 4 and 5 show the spectra of Au and Cu monitors. From these spectra, one will notice that the photopeaks characterizing the photonuclear reactions  $^{197}\text{Au}(\gamma, n)^{196g}\text{Au}$  and  $^{65}\text{Cu}(\gamma, n)^{64}\text{Cu}$  can be seen very clearly. This led to high accuracy in the data processing of the photopeaks. The areas under the photopeaks of interest were measured with relative error of less than 0.1%. The bremsstrahlung photon fluxes in the energy region from  $E_{\text{th}}$  to  $E_m$  were determined by formula (3). The total bremsstrahlung photon fluxes were determined by making the correction of the energy distributions of bremsstrahlung, which are shown in Table 5. Table 6 shows the total bremsstrahlung photon fluxes for 15, 18, 22 and 24 MeV end-point energies produced by the electron accelerator Microtron MT-25 and that of 65 MeV bremsstrahlung produced by the Pohang electron accelerator. The relative error of the total bremsstrahlung photon fluxes for both cases was less than 10%.

One can see from Table 6 that in general the total bremsstrahlung photon fluxes determined by Au and Cu monitors are in very good agreement. This fact confirms the accuracy of our method. In the previous work [27], we have determined the bremsstrahlung photon fluxes for 20 and 24 MeV end-point energies with Cu monitor. The results are also shown in Table 6.

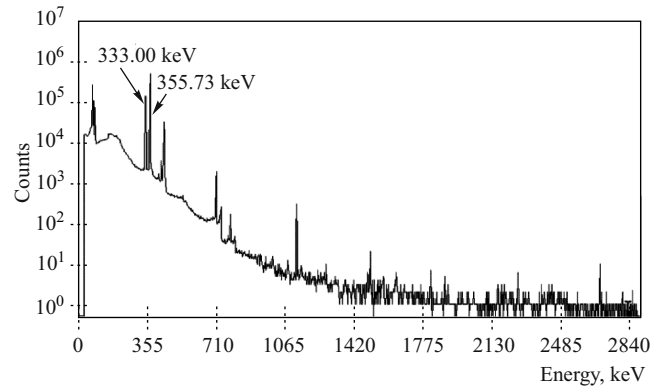


Fig. 4. Gamma spectrum of Au monitor irradiated by 18 MeV bremsstrahlung

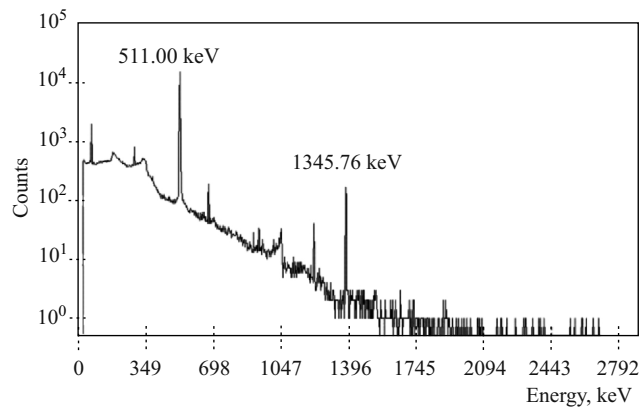


Fig. 5. Gamma spectrum of Cu monitor irradiated by 24 MeV bremsstrahlung

Table 6. The total bremsstrahlung photon fluxes at different end-point energies

Bremsstrahlung end-point energy, MeV	Total bremsstrahlung photon flux, $\text{cm}^{-2} \cdot \text{s}^{-1} \cdot \mu\text{A}^{-1}$	
	This work	References
15	$(1.530 \cdot 10^{13}) \pm 10\% ^1$	
	$(1.447 \cdot 10^{13}) \pm 10\% ^2$	
18	$(2.715 \cdot 10^{13}) \pm 10\% ^1$	
	$(2.669 \cdot 10^{13}) \pm 10\% ^2$	
20		$(3.245 \cdot 10^{13}) \pm 10\% ^2$ [27] $3.156 \cdot 10^{13}$ [29]
22	$(4.946 \cdot 10^{13}) \pm 10\% ^1$	
	$(4.797 \cdot 10^{13}) \pm 10\% ^2$	
24	$(5.628 \cdot 10^{13}) \pm 10\% ^1$	$(5.540 \cdot 10^{13}) \pm 10\% ^2$ [27]
	$(5.498 \cdot 10^{13}) \pm 10\% ^2$	
30		$6.311 \cdot 10^{13}$ [29]
60		$1.420 \cdot 10^{14}$ [29]
65	$(3.846 \cdot 10^{14}) \pm 10\% ^1$	

<sup>1</sup> Measured with Au monitor.  
<sup>2</sup> Measured with Cu monitor.

From this table one can also see that there is a good agreement between the results in the previous and present works. Because the data for the bremsstrahlung photon fluxes determined by the activation technique as shown in our work are unavailable in the current literature, we were unable to make any direct comparison with our results. Therefore, we carried out some indirect comparisons as follows. In [28] the author investigated an in vitro approach to evaluate and develop potential  $^{117m}\text{Sn}$ -based bone-seeking radiopharmaceuticals. In order to produce high specific activity  $^{117m}\text{Sn}$ , the natural tin sample was irradiated with 20 and 24 MeV end-point energies bremsstrahlung and the photonuclear reaction  $^{118}\text{Sn}(\gamma, n)^{117m}\text{Sn}$  was used. By using the data taken from their experiment and bremsstrahlung photon fluxes with end-point energies of 20 and 24 MeV produced by the Microtron in our previous work [27], the author successfully calculated the effective cross section of this reaction. Then the integrated cross sections for photonuclear reactions  $^{118}\text{Sn}(\gamma, n)^{117m}\text{Sn}$  and  $^{124}\text{Sn}(\gamma, n)^{123}\text{Sn}$  were calculated for 20 and 24 MeV bremsstrahlung end-point energies. The author saw that the integrated cross section of  $(\gamma, n)$  photonuclear reaction for  $^{118}\text{Sn}$  was approximately the same as that of  $^{124}\text{Sn}$  and in good agreement with the values obtained in our work [27]. This fact also confirms the accuracy of our results. In [29] M. J. Berger and S. M. Seltzer used the simulation method for the bremsstrahlung spectra calculation. They gave the data for the bremsstrahlung efficiency in  $[\text{photon} \cdot \text{MeV}^{-1} \cdot \text{sr}^{-1}]$ . Figure 6 [29] presents the bremsstrahlung efficiency for monoenergetic electron beams incident perpendicularly on a wolfram target. Here  $Y$  is the bremsstrahlung efficiency  $[\text{photon} \cdot \text{MeV}^{-1} \cdot \text{sr}^{-1}]$  and  $z/r_0$  is the ratio of the target thickness  $z$  and the mean range of the incident electrons  $r$ . On the basis

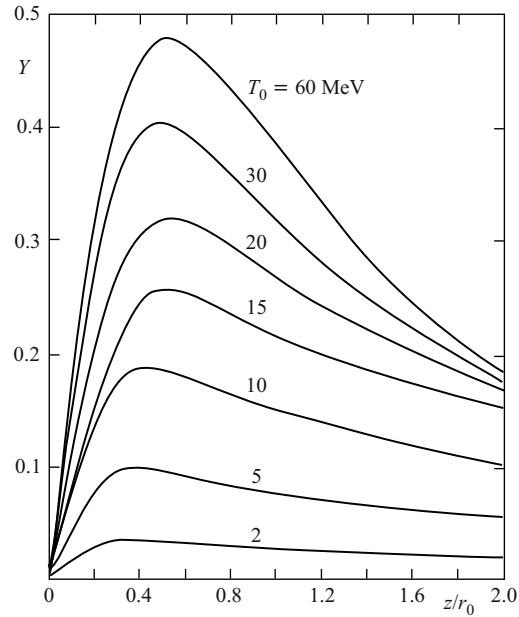


Fig. 6. Bremsstrahlung efficiency for monoenergetic electron beams incident perpendicularly on wolfram target

of the data for 20, 30 and 60 MeV end-point energies in that work (there was no available data in this work for 22, 24 and 65 MeV), we calculated the bremsstrahlung photon fluxes produced by 4 mm thick W converter (as in the case of the Microtron MT-25) for an electron beam of  $1 \mu\text{A}$ , i.e.,  $6.25 \cdot 10^{12} \text{ s}^{-1}$ . The calculated results are shown in Table 6. One can see that our experimental results and the simulation calculated results are of the same order. This fact once again confirms the accuracy of our results.

## CONCLUSIONS

The results presented in this work led to the following conclusions:

1. The bremsstrahlung photon flux increases with the end-point energies. This is logical because the probability for bremsstrahlung emission increases with kinetic energy of accelerated electron and it is well known that the kinetic energy increases with end-point energy.
2. The bremsstrahlung photon fluxes determined by Au monitor and by Cu monitor are in good agreement. This fact confirms the accuracy of our experimental results. Therefore, in this case we can determine the bremsstrahlung photon flux for a definite end-point energy as the average value of those obtained from Au and Cu monitors irradiated in the same irradiation conditions.
3. We would like also to say that the photon activation method is a good tool to determine the bremsstrahlung photon flux. In many cases it has certain advantages such as simplicity in experiment in comparison with application of ionization cameras or dosimeters as well as

accuracy in processing of photopeaks of interest. Besides, this method can be used not only for the Microtron or linear accelerator as in this work, but also for any other kind of electron accelerators and electron-bremsstrahlung converters.

**Acknowledgements.** This work has been performed at the Flerov Laboratory of Nuclear Reactions, Joint Institute for Nuclear Research, Dubna, and at the Pohang Accelerator Laboratory, Pohang, South Korea. The authors would like to express sincere thanks to the working team for operating the Microtron MT-25 and to Prof. G.N.Kim and his team for the monitor irradiation. Our thanks also go to the Chemical Department of the Flerov Laboratory of Nuclear Reactions for providing the measurement system. We are grateful to Dr. Pham Duc Khue from the Institute of Physics, VAST for the assistance in the monitor irradiation and gamma-spectra measurement at the Pohang Accelerator Laboratory. The financial support from the Vietnam National Foundation for Science and Technology Development (NAFOSTED) is highly appreciated.

#### REFERENCES

1. Berg U. E. P., Kneissl U. // Ann. Rev. Nucl. Part. Sci. 1987. V. 37. P. 33.
2. Jacobs E. et al. // Phys. Rev. C. 1980. V. 21, No. 1. P. 237.
3. Gangrski Yu. P., Tonchev A. P., Balabanov N. P. // Part. Nucl. 1996. V. 27, No. 4. P. 1043.
4. Karzmax C. J., Pering N. C. // Phys. Med. Biol. 1973. V. 18. P. 321.
5. IAEA «Manual on Radiation Sterilization of Medical and Biological Materials». Technical Report. Ser. No. 149. Vienna: IAEA, 1973.
6. Tsipenyuk Yu. M. The Microtron. London, N. Y.: Taylor & Francis, 2002. P. 167.
7. Antonov A. D. et al. JINR Preprint P15-89-318. Dubna, 1989.
8. Antonov A. D. et al. JINR Preprint P15-90-425. Dubna, 1990.
9. Do N. V. et al. // J. Kor. Phys. Soc. 2007. V. 50, No. 2. P. 417.
10. Oganessian Yu. Ts. et al. JINR Preprint E7-2000-83. Dubna, 2000.
11. Ibrahim F. et al. // Eur. Phys. J. A. 2002. V. 15. P. 357.
12. Devan K. et al. // J. Kor. Phys. Soc. 2006. V. 49, No. 1. P. 89.
13. Do N. V. et al. // Ibid. V. 48, No. 3. P. 382.
14. Kuznetsov R. A. Activation Analysis. M.: Atomizdat, 1974. P. 110.
15. Burmistenko Yu. N. Photonuclear Analysis of Compound Materials. M.: Energoatomizdat, 1986. P. 59.
16. Radiological Safety Aspects of the Operation of the Electron Linear Accelerators. Technical Report Series No. 188. Vienna: IAEA, 1979.
17. Berman B. L. // At. Nucl. Tables. 1975. V. 15. P. 319.
18. Wolfram S. Mathematica. California; N. Y.; Amsterdam; Sydney; Singapore; Tokyo; Wokingham: Wesley Publishing Comp. Inc., 1988. P. 467.
19. Lederer C. M., Shirley V. S. Table of Isotopes. 7th Ed. N. Y.; Toronto: John Wiley & Sons Inc., 1978. P. 201; 1265.
20. Firestone R. B. Table of Isotopes. CD ROM Edition, Version 1.0. Wiley Intersci., 1996. P. 1524; 8494.
21. Belov A. G. et al. JINR Preprint D15-93-80. Dubna, 1993.
22. Kim G. N. et al. // J. Kor. Phys. Soc. 2001. V. 38. P. 14.

23. *Schiff L.I.* // *Phys. Rev.* 1951. V. 83. P. 253.
24. *Khai N. T., Thiep T.D.* // *Vietnam. J. Commun. Phys.* 2003. V. 13, No. 3. P. 149.
25. *Khai N. T. et al.* // *Part. Nucl., Lett.* 2008. V. 5, No. 5. P. 736.
26. *Khai N. T. et al.* // *Part. Nucl., Lett.* 2010. V. 7, No. 1. P. 34.
27. *Thiep T.D. et al.* // *Part. Nucl., Lett.* 2005. V. 2, No. 4. P. 127.
28. *Jansen D.R.* PhD Thesis. Delft Univ. of Technology, 2010.
29. *Berger M.J., Seltzer S.M.* // *Phys. Rev. C.* 1970. V. 2, No. 2. P. 621.

Received on March 27, 2012.